DMD Fast Forward. Published on November 28, 2016 as DOI: 10.1124/dmd.116.072652
This article has not been copyedited and formatted. The final version may differ from this version.

Age-dependent absolute abundance of hepatic carboxylesterases (CES1 and CES2) by LC-MS/MS proteomics: Application to PBPK modeling of oseltamivir *in vivo* pharmacokinetics in infants

Mikael Boberg, Marc Vrana, Aanchal Mehrotra, Robin E. Pearce, Andrea Gaedigk, Deepak Kumar Bhatt, J. Steven Leeder and Bhagwat Prasad

Department of Pharmaceutics, University of Washington, Seattle, WA (M.B., M.V., A.M., D.K.B. and B.P.)

Sahlgrenska Academy, University of Gothenburg, Gothenburg, Sweden (M.B.)

Department of Clinical Pharmacology, Toxicology & Therapeutic Innovation, Children's Mercy-Kansas City, MO and School of Medicine, University of Missouri-Kansas City, Kansas City, MO (R.E.P., A.G., J.S.L.)

DMD Fast Forward. Published on November 28, 2016 as DOI: 10.1124/dmd.116.072652
This article has not been copyedited and formatted. The final version may differ from this version.

Running title: Age-dependent hepatic carboxylesterase abundance

Corresponding author: Bhagwat Prasad, Ph.D.; Department of Pharmaceutics, University of Washington, Seattle, WA 98195, Phone: (206) 221-2295, Fax: (206) 543-3204; E-mail: bhagwat@uw.edu

Number of text pages: 15

Number of tables: 3

Number of figures: 6

Number of references: 39

Number of words in Abstract: 197 (250)

Number of words in Introduction: 449 (750)

Number of words in Discussion: 951 (1,500)

Abbreviations: Area under curve (AUC), carboxylesterase (CES), drug-metabolizing enzyme (DME), maximal plasma concentration (C_{max}), pediatric physiologically based pharmacokinetic (pPBPK), pharmacokinetics (PK), multiple reaction monitoring (MRM), liquid chromatography coupled with tandem mass spectrometry (LC-MS/MS), time for maximal plasma concentration (T_{max})

ABSTRACT

The age-dependent absolute protein abundance of carboxylesterase 1 and 2 (CES1 and CES2) in human liver was investigated and applied to predict infant pharmacokinetics (PK) of oseltamivir. The CES absolute protein abundance was determined by LC-MS/MS proteomics in human liver microsomal and cytosolic fractions prepared from tissue samples obtained from 136 pediatric and 35 adult donors. Two surrogate peptides per protein were selected for the quantification of CES1 and CES2 protein abundance. Purified CES1 and CES2 protein standards were used as calibrators, and the heavy labeled peptides were used as the internal standards. In hepatic microsomes, CES1 and CES2 abundance (pmol/mg total protein) increased ~5 fold (315.2 vs. 1664.4 pmol) and ~3-fold (59.8 vs. 174.1 pmol) from neonates to adults, respectively. CES1 protein abundance in liver cytosol also showed age-dependent maturation. Oseltamivir carboxylase activity was correlated with protein expression in pediatric and adult liver microsomes. The protein abundance data were then used to model *in vivo* PK of oseltamivir in infants using pediatric physiologically based pharmacokinetic (pPBPK) modeling and incorporating the protein abundance-based ontogeny function into the existing pediatric Simcyp model. The predicted pediatric AUC, C_{max} and T_{max} were below 2.1-fold of the clinically observed values, respectively.

INTRODUCTION

Because clinical dose optimization studies often have not been conducted in children, a majority of the drugs used in pediatrics are prescribed off-label (Kimland et al., 2012; Laughon et al., 2014). This suboptimal practice could be unsafe because children, especially neonates and infants, may be susceptible to adverse drug effects or lack of drug efficacy due to their insufficient ability to metabolically eliminate or activate drugs (Hines, 2013). For example, Gray baby syndrome resulted in serious adverse effects when the antibiotic, chloramphenicol, was given to infants in whom immature glucuronidation resulted in reduced clearance of the drug (Sutherland, 1959). Therefore, the current approach to predict pediatric drug dosing, which relies on empirical body weight or body surface area normalization, should also consider the developmental trajectories of processes involved in drug disposition and response. One solution is to use pediatric physiologically based pharmacokinetic (pPBPK) models, which can be developed by integrating information on relevant age-dependent physiological differences, for dose-exposure simulations in children as an alternative to applying scaling factors to models based on adult data. In the currently available pPBPK models, different physiological factors affecting drug disposition such as organ size, tissue composition, pH in the gastrointestinal (GI) tract and body fluid dynamics are taken into consideration (Zhao et al., 2011). However, a major limitation of existing pPBPK models is the limited availability of precise developmental trajectories for major drug metabolizing enzymes (DMEs) and transporters in the drug disposition organs. Therefore, it is critical to study the developmental expression and activity of DMEs and drug transporters (Prasad et al., 2016).

Carboxylesterases (CESs) are DMEs in the alpha-beta hydrolase family, which metabolize many compounds, including drugs containing ester, thioester and amide bonds and environmental toxins such as phthalates and benzoates. Cocaine (Pindel et al., 1997), heroin (Kamendulis et al., 1996), clopidogrel (Tang et al., 2006), aspirin (Tang et al., 2006), methylphenidate (Merali et al., 2014), enalapril/ramipril (Thomsen et al., 2014), oseltamivir (Shi et al., 2006) and irinotecan (Haaz et al., 1997) are some examples of drugs and

prodrugs that undergo phase I metabolism by CESs, most of which are prescribed to children. In this study, hepatic CES1 and CES2 protein abundance in different pediatric age groups was determined and compared to the observed protein abundance in adults. While ontogeny data for hepatic CES1 and CES2 have been reported previously (Yang et al., 2009; Hines et al., 2016), we used a state-of-the-art liquid chromatography-tandem mass spectrometry (LC-MS/MS) based absolute protein quantification approach to quantify age-dependent expression of these proteins in a large cohort of well-studied pediatric and adult samples. Subsequently, the ontogeny data were incorporated into the Simcyp PBPK software (Certara Inc.) to predict *in vivo* pharmacokinetics (PK) of oseltamivir in infants.

MATERIAL AND METHODS

Materials

Synthetic heavy labeled peptides (Supplementary Table 1S) were obtained from Thermo Fisher Scientific (Rockford, IL). Chloroform, ethyl ether, Optima MS-grade acetonitrile, methanol and formic acid were purchased from Fischer Scientific (Fair Lawn, NJ). Ammonium bicarbonate (98% purity) and sodium deoxycholate (98% purity) were obtained from Thermo Fisher Scientific (Rockford, IL) and MP Biomedicals (Santa Ana, CA), respectively. CES1 and CES2 protein standards were procured from Abcam, Inc. (Cambridge, MA) and Abnova (Walnut, CA), respectively. Oseltamivir was procured from BioTang Inc., Waltham, MA.

Human liver microsomes

Thirty-five adult and seven pediatric liver tissues were procured from the liver bank of the University of Washington School of Pharmacy (Prasad et al., 2014). Procurement and storage information as well as characteristics of these tissue samples were described earlier (Paine et al., 1997). Additionally, human liver microsomal and cytosolic samples from 129

pediatric donors were obtained from the National Institute of Child Health and Human Development Brain and Tissue Bank for Developmental Disorders at the University of Maryland; the Liver Tissue Cell Distribution System, at the University of Minnesota and the University of Pittsburgh. Additional postnatal liver samples were obtained from Vitron (Tucson, AZ) and XenoTech LLC. The samples were stratified based on following age categories: neonatal (0 to 27 days; n=4), infancy (28 days to 364 days; n=17), early childhood (1 year to < 6 years; n=30), middle childhood (6 years to <12 years; n=37), adolescence (12 years to 18 years; n=48) and adulthood (>18 years; n=35) (Williams et al., 2012). The microsomal and cytosolic fractions from all samples were prepared using established protocols (Gibbs et al., 1996; Shirasaka et al., 2015; Pearce et al., 2016). Detailed donor demographic information is provided in Supplementary Table 2S. Use of these tissues has been classified as non-human subject research by the Institutional Review Boards of the University of Washington, Seattle, WA and Children's Mercy Kansas City, Kansas City, MO.

Protein denaturation, reduction, alkylation, enrichment and trypsin digestion

The purified protein standards as well as microsomal and cytosolic samples were digested by trypsin as described previously (Shirasaka et al., 2015) with few modifications. Briefly, each sample or standard was aliquoted into three tubes and individually digested using trypsin. The digested samples were processed and analyzed by LC-MS/MS on three different days to account for potential technical variability. The working calibration curve standards were prepared by diluting purified CES1 and CES2 proteins with 50 mM phosphate buffer (pH 7.4) to generate working concentrations ranging from 15 – 7680 pmol/ml (CES1; number of points on curve = 10) and 3.5 – 448 pmol/ml (CES2; number of points on curve = 8). Ten µl of the working calibration curve standards was added to 70 µl of phosphate buffer. Subsequently, 80 µl of the standard or sample (2 mg/ml) was combined with 10 µl dithiothreitol (250 mM), 40 µl ammonium bicarbonate buffer (100 mM, pH 7.8) and 20 µl deoxycholic acid (10%). Ten µl human serum albumin (10 mg/ml, for microsomal

DMD Fast Forward. Published on November 28, 2016 as DOI: 10.1124/dmd.116.072652
This article has not been copyedited and formatted. The final version may differ from this version.

samples) or 10 µl each human and bovine serum albumin (10 and 2 mg/ml, respectively, for cytosolic samples) were added as protein internal standard to address sample-to-sample variability in the trypsin digestion. The mix was then incubated at 95° for 10 minutes with gentle shaking at 300 rpm. Samples were cooled to room temperature for 10 minutes before adding 20 µl iodoacetamide (500 mM) for incubation at room temperature in the dark for 30 minutes. 500 µl ice-cold methanol, 100 µl ice-cold chloroform and 400 µl cold water were added to each sample, vortex mixed and subjected to centrifugation at 16,000 x *g* (4°C) for 5 minutes. The upper and lower layers were removed using vacuum suction and pellets were dried at room temperature for 10 minutes. Pellets were subsequently washed with 500 µl ice-cold methanol and subjected to centrifugation at 8000 x *g* (4°C) for 5 minutes after which supernatant was removed. Pellets were dried at room temperature for 30 minutes and resuspended in 60 µl ammonium bicarbonate buffer (50 mM, pH 7.8). Twenty µl of trypsin (0.16 µg/µl) was added for digestion (37°C, 16 hours, gentle shaking at 300 rpm). The trypsin digestion was quenched by placing samples on dry ice. Twenty µl of heavy peptide internal standard cocktail (dissolved in acetonitrile:water, 80:20 (v/v) with 0.5% formic acid) and ten µl acetonitrile:water 80:20 (v/v) with 0.5% formic acid were added to each sample to facilitate peptide solubility. After mixing and centrifugation at 4000 x *g* (4°C) for 5 minutes, samples were transferred to LC-MS/MS autosampler vials.

Quantitative analysis of carboxylesterases by LC-MS/MS

The LC-MS/MS system consisted of an Acquity UPLC (Waters Technologies, Milford, MA) coupled to an AB Sciex Triple Quad 6500 system (Framingham, MA) was used. Two surrogate peptides per protein were selected for the quantification of CES1 and CES2 protein abundance (Supplementary Table 1S) following previously established protocol (Prasad and Unadkat, 2014). Peptide separation was achieved on an Acquity UPLC column (HSS T3 1.8 µm. 2.1x100 mm, Waters). Mobile phases A and B consisted of water with formic acid 0.1% (v/v) and acetonitrile with formic acid 0.1% (v/v), respectively. Peptides were eluted under gradient conditions at a flow rate of 0.3 ml/min (Supplementary Table 1S).

DMD Fast Forward. Published on November 28, 2016 as DOI: 10.1124/dmd.116.072652
This article has not been copyedited and formatted. The final version may differ from this version.

Multiple reaction monitoring (MRM) conditions for targeted analysis of CES1 and CES2 surrogate peptides are provided in Supplementary Table 1S. Peak integration and quantification were performed using Analyst software (Version 1.6, Mass Spectrometry Toolkit v3.3, Framingham, MA, USA).

In vitro metabolic stability of oseltamivir

Because of the limited availability of pediatric samples, the oseltamivir depletion activity assay was only performed in a small subset of adult (n = 7) and pediatric (n = 8) samples. Oseltamivir (100 nM) was incubated at 37°C with 50 µl microsomal sample (total protein concentration, 100 µg/ml) diluted in 50 mM phosphate buffer (pH 7.4). Samples were pre-incubated at 37°C for 5 minutes before the reaction was initiated by adding 5 µl of 1 µM oseltamivir (100 nM, final concentration). The concentration of acetonitrile used to prepare oseltamivir stock solution in the *in vitro* metabolic stability assay was below 0.5% (v/v). To terminate the reaction, samples were transferred to a tube with 50 µl ice-cold acetonitrile containing internal standard diazepam (~5 ng/ml). Oseltamivir was also incubated in 50 µl of phosphate buffer at 37°C as a control for chemical degradation in the same manner. Reaction mixtures were centrifuged at 5000 x g (4°C) for 5 minutes to remove precipitated protein and supernatants transferred to LC-MS/MS autosampler vials. All *in vitro* metabolic stability assays were done in triplicate and the observed results are presented as the mean of the three analyses ± standard deviation.

LC-MS/MS method optimization and quantification of oseltamivir

LC-MS/MS system consisting of an Acquity UPLC (Waters Technologies) coupled to an AB Sciex Triple Quad 6500 system was used to quantify metabolic depletion of oseltamivir. An Acquity UPLC BEH C18 1.7 µm, 2.1x50 mm column was used with a flow rate of 0.3 ml/min and a gradient program shown in Supplementary Table 1S. The column temperature was set to 25°C. The MRM parameters for oseltamivir were *m/z* 313.3→208.2 (CE/DP, 19/56), 166.2 (CE/DP, 25/56) and 120.2 (CE/DP, 45/56). The MRM parameters for the internal

standard diazepam were *m/z* 285.1→193 and 285.1→154.0 (CE/DP, 40/100). Peak integration and quantification were performed using Analyst software (Version 1.6, Mass Spectrometry Toolkit v3.3, Framingham, MA, USA).

PBPK model development and validation for oseltamivir PK in adults

The PBPK model for oseltamivir was developed using Simcyp (Version 15, Sheffield, United Kingdom). System-dependent PBPK model parameters like organ weight, body composition and blood flow rates were already integrated into the software, while drug-dependent parameters and CES1 developmental trajectory were added to the model (Table 1). The permeability was predicted in Simcyp using the lipophilicity and polar surface area (PSA) of oseltamivir. The advanced dissolution, absorption and metabolism (ADAM) model was applied in the PBPK model. For the distribution of oseltamivir, the minimal PBPK model was used. The tissue plasma partition coefficient for liver was obtained by Poulin and Theil method prediction (Poulin and Theil, 2002). The distribution volume at steady state (V_{ss}) was estimated by fitting the model to available *in vivo* data in adults (Hu et al., 2014). For oseltamivir, CES1 was considered to be the only metabolic pathway in the model. The intrinsic clearance (CL_{int}) was extrapolated from reported *in vitro* data (Nishimuta et al., 2014). After simulation in Simcyp, the mean concentration-time profile was compared to profiles constructed from adult *in vivo* data for oseltamivir (Wattanagoon et al., 2009; Hu et al., 2014).

Extension of adult PBPK model to predict oseltamivir PK in infants (0 – 1 year of age)

Since oseltamivir is a selective CES1 substrate (Laizure SC et al., 2013), the validated adult parameters were run in the Simcyp pediatric model with the addition of age-dependent CES1 protein abundance data from this study (Table 1). A non-linear regression equation (Table 1) was used to fit the ontogeny data as described previously (Johnson et al., 2006). Since CES1 is functionally active in both microsomal and cytosolic fractions, the ontogeny equation was derived based on the total microsomal plus cytosolic abundance of CES1 per

gram of liver tissue. To do so, reported values of milligram of microsomal and cytosolic proteins per gram liver tissue (MPPGL and CPPGL, 39.8 and 80.7 mg/ml, respectively) were used to first obtain microsomal and cytosolic CES1 abundance per gram of liver (Nishimuta et al., 2014). Then, the total microsomal plus cytosolic abundance of CES1 per gram of liver tissue was derived by adding the two values. Finally, the Simcyp input values, i.e., adult normalized fractional values, were derived by considering $Adult_{max}$ equal to 1. The pediatric simulated mean concentration profile was compared to *in vivo* data in infants for oseltamivir (Kamal et al., 2014). Visual inspection and statistical analyses were conducted to assess the performance and accuracy of the pPBPK model. The pPBPK model predictions were determined to be successful if the predicted mean plasma concentration overlapped the observed *in vivo* values from the literature between the predicted 5^{th} to 95^{th} percentile interval of the plasma concentrations for oseltamivir. The mean PK parameters prediction was determined to be successful if the predicted/observed ratio for the mean PK parameters were within the 0.5 – 2 ratio window.

Statistical analysis

Non-parametric tests were used to test age- or genotype-dependence. For individual categories (neonates to adults), age-dependent data analysis was performed using the Kruskal-Wallis test followed by Dunn's multiple comparison test. To compare two groups (e.g., the effects of gender, ethnicity or variant alleles) the Mann-Whitney test was used. A non-linear regression model with baseline protein abundance (Table 1) (GraphPad Prism, San Diego, California) was fitted to the continuous ontogenic protein abundance data. The goodness of model fit was evaluated by visual inspection, 95% confidence intervals (CIs) of the parameter estimates and residual plots. Weights of $1/Y^2$ were used. For correlation analysis, the non-parametric Spearman regression test was used because the data were asymmetrically distributed. A *p*-value below 0.05 was considered to be statistically significant. The observed data was illustrated in graphs and tables using Microsoft Excel (Version 14, Redmond, WA, USA) and GraphPad Prism.

RESULTS

Age-dependent protein abundance of CES1 and CES2

Two different peptides of both CES1 and CES2 showed excellent correlation (r^2 > 0.9) indicating the robustness of absolute protein quantification by LC-MS/MS (Fig. 1). The lower limit of quantification of CES1 and CES2 was 0.15 and 0.35 fmol (on column), respectively. Both the absolute abundance and interindividual variability of CES1 in liver were higher than CES2. For example, CES1 was 9.6-fold higher than CES2 in adult human liver microsomes (1664.4 ± 781.7 and 174.1 ± 105.7 pmol/mg microsomal protein, respectively; Table 2). CES1 abundance was more variable (25.4 to 4015.4 pmol/mg microsomal protein; 158.1-fold variability) compared to CES2 (15.6 to 527.3 pmol/mg microsomal protein; 33.8-fold variability). To investigate the factors affecting protein abundance of CES1 and CES2, the data were stratified and analyzed based on age, gender and ethnicity. Non-linear regression of the microsomal protein abundance data revealed that expression of CES1 and CES2 protein was 50% of the values observed in adults (Age50) by approximately 7.4 months (0.62 years) and 3 weeks (0.06 years), respectively. The exponential factor (n, arbitrary units) describing the developmental curve for CES1 and CES2 was similar, 0.53 vs. 0.59, respectively. Stratifying by age as a categorical variable, the microsomal CES1 protein abundance was 5.3-fold ($p < 0.0001$) higher in adults compared to neonates (Fig. 2, Table 2). Similarly, neonatal CES1 abundance was significantly lower compared to that observed in early childhood, middle childhood and adolescence (Fig. 2). Furthermore, microsomal CES1 abundance was lower in infants compared to early childhood, middle childhood, adolescence and adulthood. The average absolute cytosolic content of CES1 (pmol/mg protein) was 3.2 fold lower than the microsomal abundance across the entire age range (Fig. 3A and Table 2). Cytosolic hepatic CES1 expression levels were also age-dependent as evidenced by a 3.1-fold difference between neonatal and adult samples (Fig 3B). Because of the limited availability of pediatric samples, the esterase activity assay was only conducted in a subset of samples. A 2.4-fold difference ($p < 0.05$) in oseltamivir biotransformation was observed among adult (n = 7) and pediatric samples (n = 8) (relative rate of elimination (*k)* of

DMD Fast Forward. Published on November 28, 2016 as DOI: 10.1124/dmd.116.072652
This article has not been copyedited and formatted. The final version may differ from this version.

61.7 ± 32.9 and 25.9 ± 22.3 min^{-1}, respectively) (Fig. 4). A correlation was observed between CES1 protein abundance and hepatic esterase activity (r = 0.64, Spearman correlation, $p < 0.05$). CES2 expression was also found to be age-dependent, albeit the difference was only observed between the neonate and adolescent age groups. No significant difference in CES2 protein abundance was observed between other groups (Fig. 2). Taken together, the relative ratio of CES1:CES2 in liver microsomes increases during human development with relative percentages of 84:16 (neonates and infants) to 91:9 (adults) (Supplementary Fig. 1S). No effect of gender or ethnicity were observed on CES1 and CES2 protein abundance (Supplementary Fig. 2S). The CES2 peptides could not be reliably quantified in the cytosolic fractions because of low protein abundance.

Correlation of CES1 and CES2 protein abundance

CES1 and CES2 protein abundances were significantly correlated across the entire pediatric and adult cohorts (r^2 = 0.49, Spearman correlation, p value <0.05). As shown in Fig. 5, higher CES1 protein abundance was associated with higher CES2 protein abundance suggesting that CES1 and CES2 expression may be co-regulated. Interestingly, the correlation between these proteins was stronger in the younger age groups compared to adults (Supplementary Fig. 3S). The slopes were slightly different between age groups; however, a larger number of samples are needed to confirm the age-related differences in the regulation of CES1 and CES2.

pPBPK modeling predictions for oseltamivir disposition in adults and infants

The predicted mean plasma concentration of oseltamivir in adults and infants after 150 mg and 3 mg/kg oral administration are shown in Fig. 6A and 6B, respectively. These predicted curves were similar to those previously observed in clinical data (Wattanagoon et al., 2009; Hu et al., 2014; Kamal et al., 2014). The prediction of the mean PK parameters, area under

curve (AUC), maximal plasma concentration (C_{max}) and time for maximal plasma concentration (T_{max}) were within a 0.5 – 2.1-fold window of the observed data (Table 3).

DISCUSSION

Although CES1 and CES2 protein expression data have been reported previously (Yang et al., 2009; Hines et al., 2016), our data present absolute protein quantification by LC-MS/MS methodology in a large cohort of well-characterized pediatric as well as adult samples. Compared to traditional immuno-quantification, LC-MS/MS proteomics has emerged as a superior protein quantification method (Aebersold et al., 2013). LC-MS/MS proteomics offers many advantages such as selectivity, precision, accuracy and short analysis time. Additionally, the correlation between multiple peptides per protein indicates the robustness of this method. At an absolute level, CES1 was found to be one of the most highly expressed DMEs in the liver. For example, CES1 abundance in the liver is ~20 to 30-fold higher than the most abundant adult cytochrome P450 enzyme, CYP3A4 (Achour et al., 2014). Interestingly, while the absolute abundance values of CES1 and CES2 presented in this study are consistent with those reported by other LC-MS/MS proteomics studies (Sato et al., 2012; Wang et al., 2016), the values reported by Hines et al. are significantly lower, which might be due to the methodological differences, i.e. LC-MS/MS proteomics vs. immunoblotting.

Irrespective of the absolute values, our results are consistent with reported data regarding an age-related relative increase of CES1 and CES2. Hines et al. recently reported that CES1 and CES2 expression increases rapidly after birth with median microsomal CES1 content lower among samples from subjects younger than 3 weeks (n = 36) compared with subjects older than 3 weeks to 18 years (6.27 vs. 17.5 pmol/mg microsomal protein, respectively). Similarly, CES2 microsomal content was reported as 1.8, 2.9, and 4.2 pmol/mg microsomal protein, in samples from donors younger than 3 weeks, 3 weeks to 6 years and 6 years to 18 years, respectively, using classification tree analysis to determine

the age-related breakpoints in the developmental trajectories (Hines et al., 2016). 319-fold and 55-fold lower mRNA expression levels of CES1 and CES2, respectively, were observed in fetal liver samples as compared to adult liver samples (Yang et al., 2009). In a limited number of liver tissue samples from children between 0 and 10 years of age, the observed CES1 protein expression was 4-fold lower than in adult samples (Yang et al., 2009). Consistent with our data, Shi et al. (Shi et al., 2011) and Chen et al. (Chen et al., 2015) have also reported age-dependent relative changes in CES1 and CES2 hepatic activity. The suggested variability in age-dependent CES1 protein expression level is confirmed in this study and compared with the adult data. However, the combination of absolute protein quantitation and a relatively large samples number together with non-linear regression analysis allowed us to investigate in more detail the actual developmental trajectory for postnatal CES expression, with the microsomal CES1 expression reaching levels half that observed in adults by approximately 7 months of age, and CES2 expression reaching the same level much earlier, at 3 weeks of age. Since there was no association between gender or ethnicity and CES1 and CES2 protein abundance, these factors are unlikely to confound data interpretation.

The correlation of CES1 and CES2 protein abundances suggests that expression of these enzymes is likely to be co-regulated, where these enzymes are either induced or suppressed by at least one similar molecular mechanism. The co-regulation mechanism(s) of *CES* gene expression is still unknown. However, both genes are located in close proximity to one another on chromosome 16 (*CES1* on Ch16q12.2 and *CES2* at Ch16q22.1 (Langmann et al., 1997; Merali et al., 2014)) which might explain co-regulation of the expression of the two CES proteins. The knowledge about co-regulated expression of DMEs is important for PBPK modeling (Achour et al., 2014).

The protein abundance data of CES1, when integrated into a pPBPK model, predicted the majority of oseltamivir PK data in infants. Such an ontogeny-based approach has been

successfully used recently to predict pediatric drug disposition of acetaminophen (Jiang et al., 2013). Taken together, the CES1 absolute ontogeny data presented here show a difference in the prodrug metabolizing capacities of neonates and infants versus older children and adults. CES ontogeny-based pPBPK models can be used to predict the first-in-child dose of prodrugs and ester/amide drugs to minimize the risk of toxicities and avoid unnecessary drug exposure in this vulnerable population. In general, esters are prone to penetration across the blood-brain barrier as compared to their acid metabolites. Therefore, a better understanding of CES ontogeny can predict neurological adverse effects in children, as reported in the case of oseltamivir (Dalvi et al., 2011). Moreover, ontogeny-based pPBPK-models can also be used to predict exposure and detoxification mechanisms for ester- or amide-based environmental toxins, such as pesticides and flame retardants.

Our study has a few limitations. For instance, neonatal data should be interpreted with caution because we were only able to obtain four samples from the age group up to 27 days. Further studies are also warranted to investigate the mechanisms co-regulating CES1 and CES2 protein expression and to determine the its biological significance. Finally, some of the observed data points (Fig. 6B) were below the 5% or above the 95% confidence interval, suggesting that a pPBPK model based on sparse activity data is inadequate to model oseltamivir PK in this age group. It is also possible that other esterase pathways may be involved in oseltamivir elimination, or CES1 or CES2 expression in extrahepatic tissues may contribute to oseltamivir clearance.

In summary, CES1 is a major esterase enzyme in the liver with 9.6-fold higher abundance than CES2. CES1 is also more variable than CES2 and the ontogeny is one of the significant contributors to the observed variability. These data will be useful to derive scaling factors to predict age-dependent hepatic clearance of CES substrates via pPBPK modeling and simulations.

ACKNOWLEDGEMENT

Prachi Jha, Department of Pharmaceutics, University of Washington assisted with LC-MS/MS data analysis.

AUTHORSHIP CONTRIBUTIONS

Participated in research design: M.B, M.V., R.E.P., A.G., J.S.L., B.P.

Conducted experiments: M.B, M.V., A.M., D.K.B., B.P.

Performed data analysis: M.B, M.V., A.M., D.K.B., B.P.

Wrote or contributed to the writing of the manuscript: M.B, M.V., A.M., R.E.P., A.G., D.K.B., J.S.L., B.P.

REFERENCES

Achour B, Russell MR, Barber J and Rostami-Hodjegan A (2014) Simultaneous quantification of the abundance of several cytochrome P450 and uridine 5'-diphospho-glucuronosyltransferase enzymes in human liver microsomes using multiplexed targeted proteomics. *Drug Metab Dispos* **42**:500-510.

Aebersold R, Burlingame AL and Bradshaw RA (2013) Western blots versus selected reaction monitoring assays: time to turn the tables? *Mol Cell Proteomics* **12**:2381-2382.

Chen YT, Trzoss L, Yang D and Yan B (2015) Ontogenic expression of human carboxylesterase-2 and cytochrome P450 3A4 in liver and duodenum: postnatal surge and organ-dependent regulation. *Toxicology* **330**:55-61.

Dalvi PS, Singh A, Trivedi HR, Mistry SD and Vyas BR (2011) Adverse drug reaction profile of oseltamivir in children. *J Pharmacol Pharmacother* **2**:100-103.

Gibbs JP, Czerwinski M and Slattery JT (1996) Busulfan-glutathione conjugation catalyzed by human liver cytosolic glutathione S-transferases. *Cancer Res* **56**:3678-3681.

Haaz MC, Rivory LP, Riche C and Robert J (1997) The transformation of irinotecan (CPT-11) to its active metabolite SN-38 by human liver microsomes. Differential hydrolysis for the lactone and carboxylate forms. *Naunyn Schmiedebergs Arch Pharmacol* **356**:257-262.

Hines RN, Simpson PM and McCarver DG (2016) Age-Dependent Human Hepatic Carboxylesterase 1 (CES1) and Carboxylesterase 2 (CES2) Postnatal Ontogeny. *Drug Metab Dispos* **44**:959-966.

Hu ZY, Edginton AN, Laizure SC and Parker RB (2014) Physiologically based pharmacokinetic modeling of impaired carboxylesterase-1 activity: effects on oseltamivir disposition. *Clin Pharmacokinet* **53**:825-836.

Instiaty I, Lindegardh N, Jittmala P, Hanpithakpong W, Blessborn D, Pukrittayakamee S, White NJ and Tarning J (2013) Comparison of oseltamivir and oseltamivir carboxylate concentrations in venous plasma, venous blood, and capillary blood in healthy volunteers. *Antimicrob Agents Chemother* **57**:2858-2862.

Jiang XL, Zhao P, Barrett JS, Lesko LJ and Schmidt S (2013) Application of physiologically based pharmacokinetic modeling to predict acetaminophen metabolism and pharmacokinetics in children. *CPT Pharmacometrics Syst Pharmacol* **2**:e80.

Johnson TN, Rostami-Hodjegan A and Tucker GT (2006) Prediction of the clearance of eleven drugs and associated variability in neonates, infants and children. *Clin Pharmacokinet* **45**:931-956.

Kamal MA, Acosta EP, Kimberlin DW, Gibiansky L, Jester P, Niranjan V, Rath B, Clinch B, Sanchez PJ, Ampofo K, Whitley R and Rayner CR (2014) The posology of oseltamivir in infants with influenza infection using a population pharmacokinetic approach. *Clin Pharmacol Ther* **96**:380-389.

Kamendulis LM, Brzezinski MR, Pindel EV, Bosron WF and Dean RA (1996) Metabolism of cocaine and heroin is catalyzed by the same human liver carboxylesterases. *J Pharmacol Exp Ther* **279**:713-717.

Kimland E, Nydert P, Odlind V, Bottiger Y and Lindemalm S (2012) Paediatric drug use with focus on off-label prescriptions at Swedish hospitals - a nationwide study. *Acta Paediatr* **101**:772-778.

Laizure SC, Herring V, Hu Z, Witbrodt K and RB. P (2013) The Role of Human Carboxylesterases in Drug Metabolism: Have We Overlooked Their Importance. *Pharmacotherapy* **33**:210-222.

Langmann T, Becker A, Aslanidis C, Notka F, Ullrich H, Schwer H and Schmitz G (1997) Structural organization and characterization of the promoter region of a human carboxylesterase gene. *Biochim Biophys Acta* **1350**:65-74.

Laughon MM, Avant D, Tripathi N, Hornik CP, Cohen-Wolkowiez M, Clark RH, Smith PB and Rodriguez W (2014) Drug labeling and exposure in neonates. *JAMA Pediatr* **168**:130-136.

Merali Z, Ross S and Pare G (2014) The pharmacogenetics of carboxylesterases: CES1 and CES2 genetic variants and their clinical effect. *Drug Metabol Drug Interact* **29**:143-151.

Nishimuta H, Houston JB and Galetin A (2014) Hepatic, intestinal, renal, and plasma hydrolysis of prodrugs in human, cynomolgus monkey, dog, and rat: implications for in vitro-in vivo extrapolation of clearance of prodrugs. *Drug Metab Dispos* **42**:1522-1531.

Paine MF, Khalighi M, Fisher JM, Shen DD, Kunze KL, Marsh CL, Perkins JD and Thummel KE (1997) Characterization of interintestinal and intraintestinal variations in human CYP3A-dependent metabolism. *J Pharmacol Exp Ther* **283**:1552-1562.

Parrott N, Davies B, Hoffmann G, Koerner A, Lave T, Prinssen E, Theogaraj E and Singer T (2011) Development of a physiologically based model for oseltamivir and simulation of pharmacokinetics in neonates and infants. *Clin Pharmacokinet* **50**:613-623.

Pearce RE, Gaedigk R, Twist GP, Dai H, Riffel AK, Leeder JS and Gaedigk A (2016) Developmental Expression of CYP2B6: A Comprehensive Analysis of mRNA Expression, Protein Content and Bupropion Hydroxylase Activity and the Impact of Genetic Variation. *Drug Metab Dispos* **44**:948-958.

Pindel EV, Kedishvili NY, Abraham TL, Brzezinski MR, Zhang J, Dean RA and Bosron WF (1997) Purification and cloning of a broad substrate specificity human liver carboxylesterase that catalyzes the hydrolysis of cocaine and heroin. *J Biol Chem* **272**:14769-14775.

Poulin P and Theil FP (2002) Prediction of pharmacokinetics prior to in vivo studies. 1. Mechanism-based prediction of volume of distribution. *J Pharm Sci* **91**:129-156.

Prasad B, Evers R, Gupta A, Hop CE, Salphati L, Shukla S, Ambudkar SV and Unadkat JD (2014) Interindividual variability in hepatic organic anion-transporting polypeptides and P-glycoprotein (ABCB1) protein expression: quantification by liquid chromatography tandem mass spectroscopy and influence of genotype, age, and sex. *Drug Metab Dispos* **42**:78-88.

Prasad B, Gaedigk A, Vrana M, Gaedigk R, Leeder JS, Salphati L, Chu X, Xiao G, Hop CE, Evers R, Gan L and Unadkat JD (2016) Ontogeny of hepatic drug transporters as quantified by LC-MS/MS proteomics. *Clin Pharmacol Ther*.

Prasad B and Unadkat JD (2014) Optimized approaches for quantification of drug transporters in tissues and cells by MRM proteomics. *AAPS J* **16**:634-648.

Sato Y, Miyashita A, Iwatsubo T and Usui T (2012) Simultaneous absolute protein quantification of carboxylesterases 1 and 2 in human liver tissue fractions using liquid chromatography-tandem mass spectrometry. *Drug Metab Dispos* **40**:1389-1396.

Shi D, Yang D, Prinssen EP, Davies BE and Yan B (2011) Surge in expression of carboxylesterase 1 during the post-neonatal stage enables a rapid gain of the

capacity to activate the anti-influenza prodrug oseltamivir. *J Infect Dis* **203**:937-942.

Shi D, Yang J, Yang D, LeCluyse EL, Black C, You L, Akhlaghi F and Yan B (2006) Anti-influenza prodrug oseltamivir is activated by carboxylesterase human carboxylesterase 1, and the activation is inhibited by antiplatelet agent clopidogrel. *J Pharmacol Exp Ther* **319**:1477-1484.

Shirasaka Y, Chaudhry AS, McDonald M, Prasad B, Wong T, Calamia JC, Fohner A, Thornton TA, Isoherranen N, Unadkat JD, Rettie AE, Schuetz EG and Thummel KE (2015) Interindividual variability of CYP2C19-catalyzed drug metabolism due to differences in gene diplotypes and cytochrome P450 oxidoreductase content. *Pharmacogenomics J*.

Tang M, Mukundan M, Yang J, Charpentier N, LeCluyse EL, Black C, Yang D, Shi D and Yan B (2006) Antiplatelet agents aspirin and clopidogrel are hydrolyzed by distinct carboxylesterases, and clopidogrel is transesterificated in the presence of ethyl alcohol. *J Pharmacol Exp Ther* **319**:1467-1476.

Thomsen R, Rasmussen HB, Linnet K and Consortium I (2014) In vitro drug metabolism by human carboxylesterase 1: focus on angiotensin-converting enzyme inhibitors. *Drug Metab Dispos* **42**:126-133.

Wang X, Liang Y, Liu L, Shi J and Zhu HJ (2016) Targeted absolute quantitative proteomics with SILAC internal standards and unlabeled full-length protein calibrators (TAQSI). *Rapid Commun Mass Spectrom* **30**:553-561.

Wattanagoon Y, Stepniewska K, Lindegardh N, Pukrittayakamee S, Silachamroon U, Piyaphanee W, Singtoroj T, Hanpithakpong W, Davies G, Tarning J, Pongtavornpinyo W, Fukuda C, Singhasivanon P, Day NP and White NJ (2009) Pharmacokinetics of high-dose oseltamivir in healthy volunteers. *Antimicrob Agents Chemother* **53**:945-952.

Williams K, Thomson D, Seto I, Contopoulos-Ioannidis DG, Ioannidis JP, Curtis S, Constantin E, Batmanabane G, Hartling L, Klassen T and Sta RCHG (2012) Standard 6: age groups for pediatric trials. *Pediatrics* **129 Suppl 3**:S153-160.

Yang D, Pearce RE, Wang X, Gaedigk R, Wan YJ and Yan B (2009) Human carboxylesterases HCE1 and HCE2: ontogenic expression, inter-individual variability and differential hydrolysis of oseltamivir, aspirin, deltamethrin and permethrin. *Biochem Pharmacol* **77**:238-247.

Zhao P, Zhang L, Grillo JA, Liu Q, Bullock JM, Moon YJ, Song P, Brar SS, Madabushi R, Wu TC, Booth BP, Rahman NA, Reynolds KS, Gil Berglund E, Lesko LJ and Huang SM (2011) Applications of physiologically based pharmacokinetic (PBPK) modeling and simulation during regulatory review. *Clin Pharmacol Ther* **89**:259-267.

FOOTNOTES

Mikael Boberg and Marc Vrana contributed equally.

The study was supported by the Eunice Kennedy Shriver National Institute of Child Health & Human Development of the National Institutes of Health [Award: NICHD R01HD081299]. The Liver Tissue Cell Distribution System is funded by the National Institutes of Health [Contract N01-DK-7-0004/HHSN267200700004C]. The project, entitled "Laboratory of Developmental Biology," was supported by an award from the Eunice Kennedy Shriver National Institute of Child Health & Human Development of the National Institutes of Health [Award 5R24HD0008836].

Human liver microsomal and cytosolic samples from pediatric donors were obtained from the National Institute of Child Health and Human Development Brain and Tissue Bank for Developmental Disorders at the University of Maryland [funded by National Institutes of Health (NIH) contract HHSN275200900011C, reference number, N01-HD-9-0011]; the Liver Tissue Cell Distribution System [funded by NIH contract number, N01-DK-7-0004/HHSN267200700004C], at the University of Minnesota and the University of Pittsburgh.

FIGURE LEGENDS

Fig. 1: Correlation between two peptides for CES1 (A) and CES2 (B) used for absolute protein quantification (pmol/mg microsomal proteins)

Fig. 2: Hepatic microsomal CES1 and CES2 protein abundance during human development (categorical (A) and continuous (B)). Age classification: neonatal (0 to 27 days), infancy (28 days to 364 days), early childhood (1 year to < 6 years), middle childhood (6 years to < 12 years), adolescence (12 years to 18 years) and adulthood (>18 years). The number of subjects in each age category are indicated in parentheses in the x-axis of categorical data. Dot plots are displayed with mean protein abundance as the horizontal line. The error bar displays SD with individual maximum and minimum values shown in the dot plot. *, ** and *** indicate *p* values of <0.05, <0.001 and <0.0001, respectively.

Fig. 3: Hepatic cytosolic CES1 protein abundance in different age categories (A) and correlation of microsomal (Fig. 2) and cytosolic CES1 protein abundance (B). Age classification: neonatal (0 to 27 days), infancy (28 days to 364 days), early childhood (1 year to < 6 years), middle childhood (6 years to < 12 years), adolescence (12 years to 18 years) and adulthood (>18 years). Dot plots are displayed with mean protein abundance as the horizontal line. The error bar displays SD with individual maximum and minimum values shown in the dot plot. * and *** indicate p-values of <0.05 and <0.0001, respectively.

Fig. 4: Oseltamivir activity in representative adult (n = 7) and pediatric (n = 8) samples. CES1 activity was determined using oseltamivir metabolism to the corresponding carboxylate.

Fig. 5: Correlation of CES1 and CES2 protein abundance in human liver microsomes. The correlation was determined as significant by a Spearman correlation test (p < 0.0001).

Fig. 6: Mean predicted systemic concentration of oseltamivir (black line) in adults after 150 mg oral administration (A) and infants after 3 mg/kg oral administration (B) with the predicted 5th and 95th percentiles confidence intervals (dotted lines) plotted. The circles represent the observed *in vivo* values from the literature. The observed *in vivo* values were inside the predicted 5th to 95th percentile interval for adults. Some of the observed pediatric values are below 5^{th} percentile and above the 95^{th} percentile of the predicted values.

DMD Fast Forward. Published on November 28, 2016 as DOI: 10.1124/dmd.116.072652
This article has not been copyedited and formatted. The final version may differ from this version.

TABLES

Table 1: Physicochemical properties, absorption, distribution and elimination used for oseltamivir PBPK model development. The observed differences between the pediatric and adult CL_{int} are assumed to be due to the differences in V_{max}, which are extrapolated from the obtained CES abundance data in pediatric subjects

Parameter	Oseltamivir	Reference
Physicochemical properties		
Molecular weight (g/mol)	312.4	
LogD at pH 7.4	0.36	(Parrott et al., 2011)
pKa	7.75	
Fraction unbound	0.58	(Hu et al., 2014)
Blood-to-plasma ratio	1.42	(Instiaty et al., 2013)
Absorption		
Absorption model	ADAM model	
Cell permeability (10^{-4} cm/s)	0.8	Simcyp (fitted)
Distribution		
Distribution model	Minimal PBPK model	
V_{ss} (l/kg)	3.4	Simcyp (fitted)
Elimination		
Clearance type	Whole organ metabolic Clearance	
CL_{int} in S9 fraction, adults (µl/min/mg protein)	67	(Nishimuta et al., 2014)
CL_{renal}, adults	29	US-FDA (http://www.accessdata.fda.gov/drugsatfda_docs/nda/99/21087_Tamiflu_bior.pdf)
Ontogeny equation*	$F = \left(\frac{Adult_{max} - F_{birth}}{Age50^{n} + Age^{n}}\right) \times Age^{n} + F_{birth}$	
CES1 ontogeny parameters*	F_{birth}, $Adult_{max}$, Age_{50} and n = 0.20, 1, 1.10 and 0.56, respectively[#]	Present study

*F, fractional protein abundance in adult samples; $Adult_{max}$, maximum average relative protein abundance; F_{birth}, fractional protein abundance (of adult) at birth; Age50, age in years at which half-maximum adult protein abundance is obtained; Age, age in years of the subject at the time of sample collection; n, exponential factor.

[#]Since CES1 is functionally active in both microsomal and cytosolic fractions, the ontogeny equation was derived based on the total microsomal plus cytosolic abundance of CES1 per gram of liver tissue. To do so, reported values of milligram of microsomal and cytosolic proteins per gram liver tissue (MPPGL and CPPGL, 39.8 and 80.7 mg/ml, respectively) were used to first obtain microsomal and cytosolic CES1 abundance per gram of liver. Then, total microsomal plus cytosolic abundance of CES1 per gram of liver tissue was derived by adding the two values. Finally, the adult normalized fractional values were derived by considering $Adult_{max}$ equal to 1.

DMD Fast Forward. Published on November 28, 2016 as DOI: 10.1124/dmd.116.072652
This article has not been copyedited and formatted. The final version may differ from this version.

Table 2: Age-dependent protein abundance (pmol/mg total protein, mean ± SD) of CES1, CES2 and total CES1+CES2 in human liver microsomes and cytosols.

Age category	CES1		CES2	CES1 + CES2
	Microsomal	Cytosolic	Microsomal	Microsomal
Neonatal	315.2 ± 241.1	184.2 ± 150.9	59.8 ± 26.2	374.9 ± 266.4
Infancy	722.2 ± 535.9	255.7 ± 184.0	134.3 ± 91.4	856.5 ± 614.2
Early childhood	1262.1 ± 434.3	288.0 ± 168.4	154.4 ± 71.4	1416.5 ± 488.8
Middle childhood	1216.5 ± 448.4	351.5 ± 265.6	155.6 ± 60.8	1372.1 ± 498.7
Adolescence	1261.5 ± 469.5	495.5 ± 241.6	165.2 ± 72.0	1426.7 ± 524.4
Adulthood	1664.4 ± 781.7	556.5 ± 311.1	174.1 ± 105.7	1829.1 ± 856.2

DMD Fast Forward. Published on November 28, 2016 as DOI: 10.1124/dmd.116.072652
This article has not been copyedited and formatted. The final version may differ from this version.

Table 3: The virtual clinical trials design and observed and predicted mean PK parameters for oseltamivir in adults and infants

Virtual clinical trial design		
Parameter		
Population type	Healthy adult volunteers	Pediatric
Maximum age (years)	45	1
Minimum age (years)	18	0
Number of trials	10	10
Number of subjects per trial	10	10
Total number of subjects	100	100
Study duration (hours)	13	13
Number of time samples	200	200
Dose	150 mg	3 mg/kg
Dosing regimen	Single dose	Single dose
Fluid intake with dose (ml)	250	100
Fasted or fed	Fasted	Fasted

Mean PK parameters for oseltamivir in adults			
Mean PK parameter	**Observed**	**Predicted**	**Predicted/Observed ratio**
AUC (ng/ml×h)	297	270	1.1
C_{max} (ng/ml)	99	117	0.9
T_{max} (h)	0.95	0.77	1.2

Mean PK parameters for oseltamivir in infants			
Mean PK parameter	**Observed**	**Predicted**	**Predicted/Observed ratio**
AUC (ng/ml×h)	308	566	1.8
C_{max} (ng/ml)	78	166	2.1
T_{max} (h)	0.9	1.17	1.3

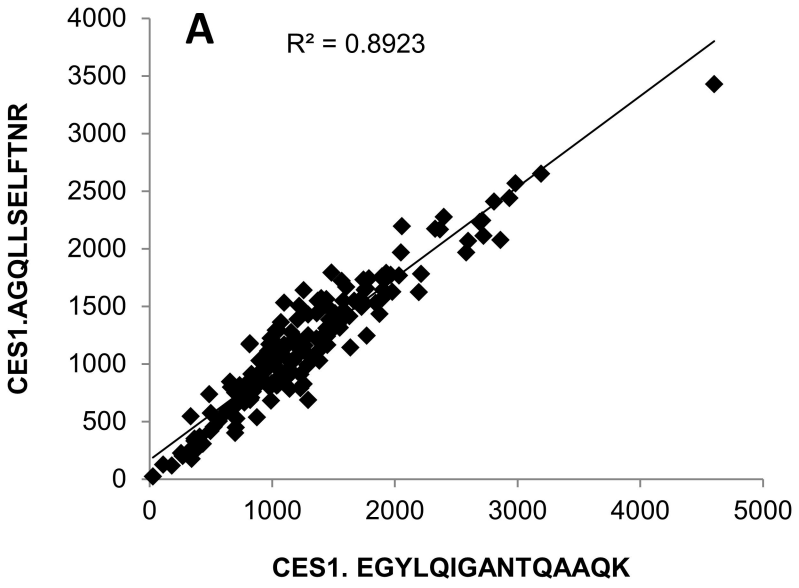

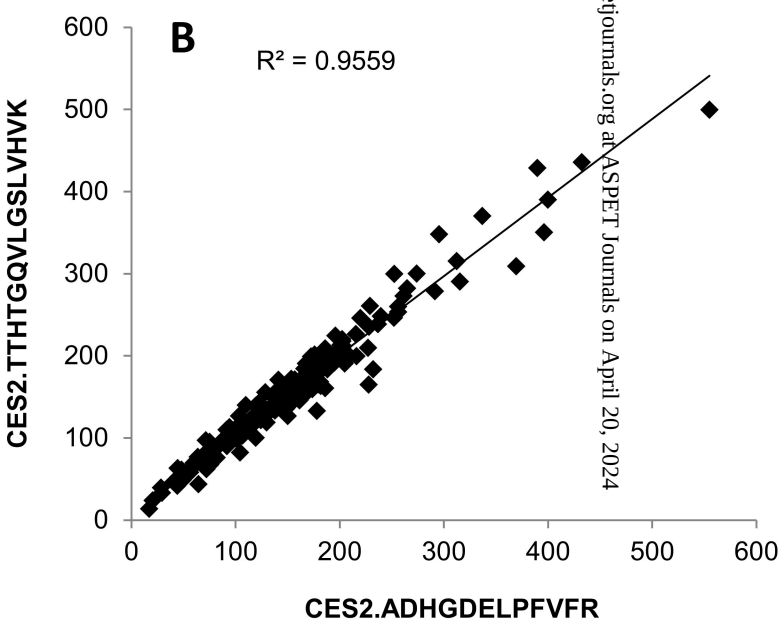

Fig. 1.

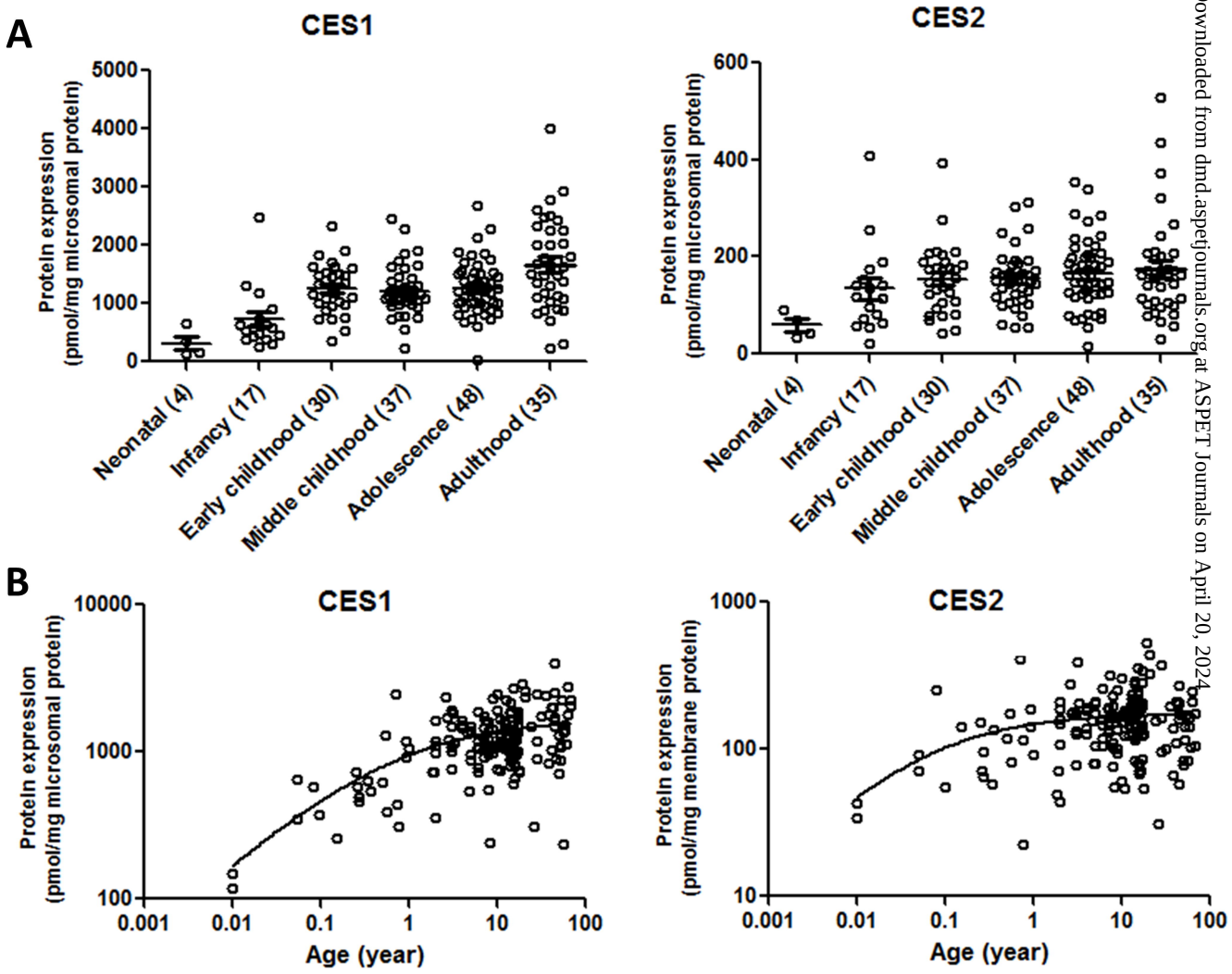

	CES1	CES2
Neonatal vs. Early childhood	*	
Neonatal vs. Adolescence	*	*
Neonatal vs. Adulthood	**	
Infancy vs. Early childhood or adolescence	**	
Infancy vs. Middle childhood	*	
Infancy vs. Adulthood	***	

Fig. 2.

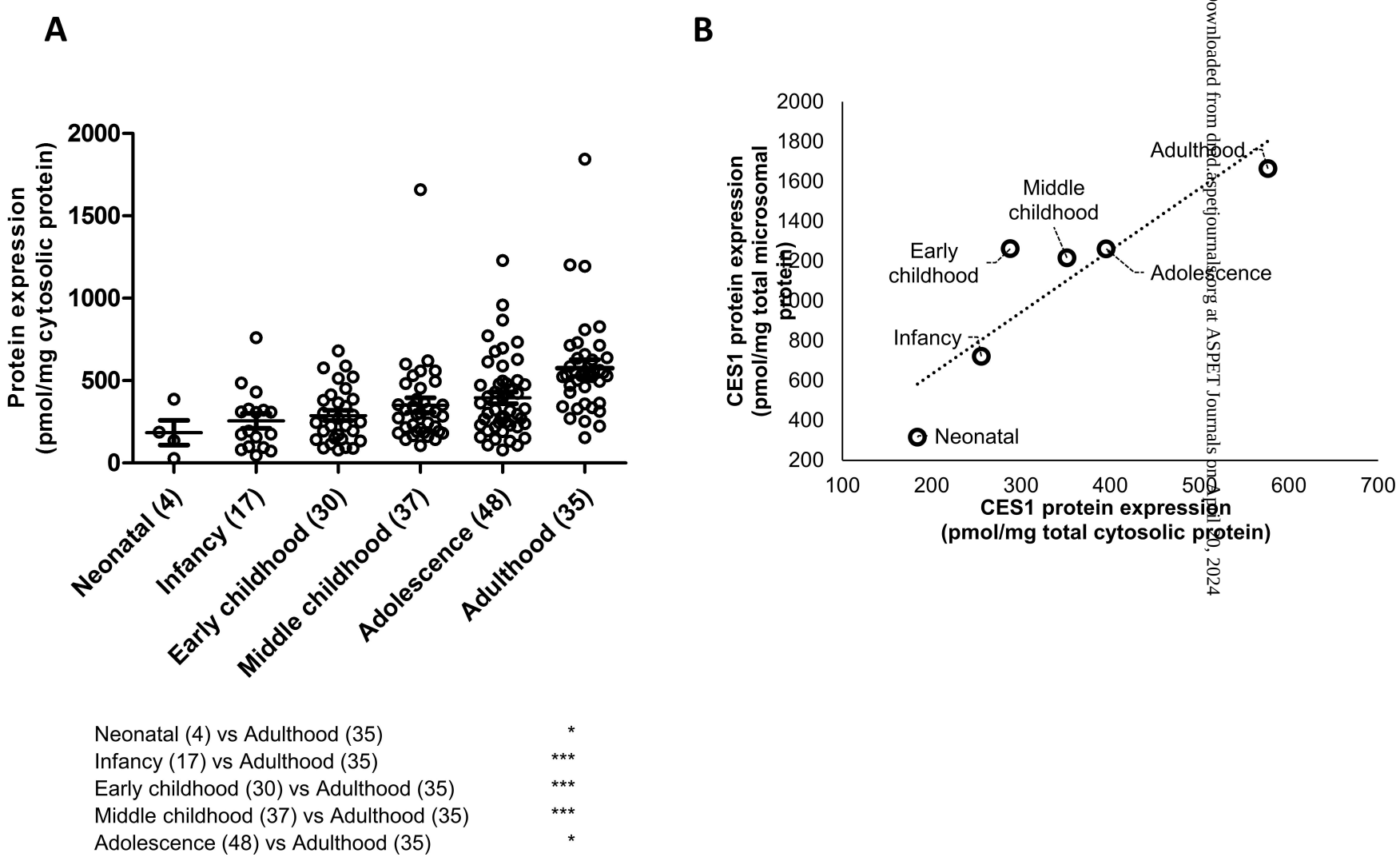

Fig. 3.

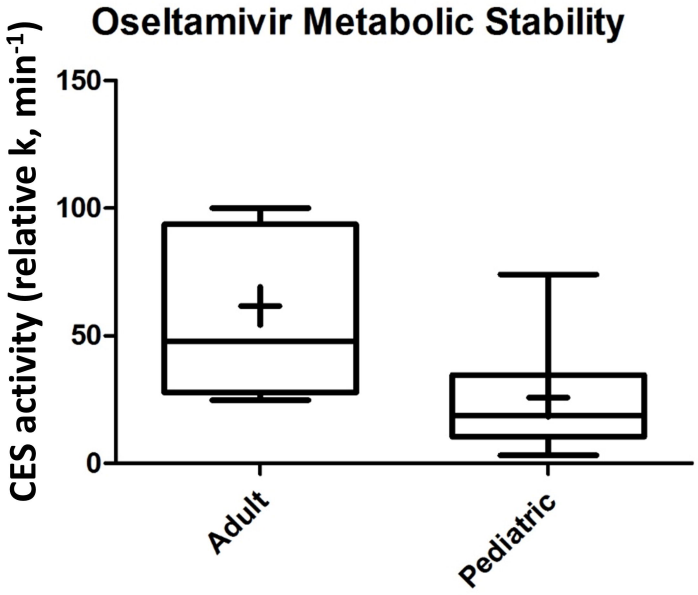

Fig. 4.

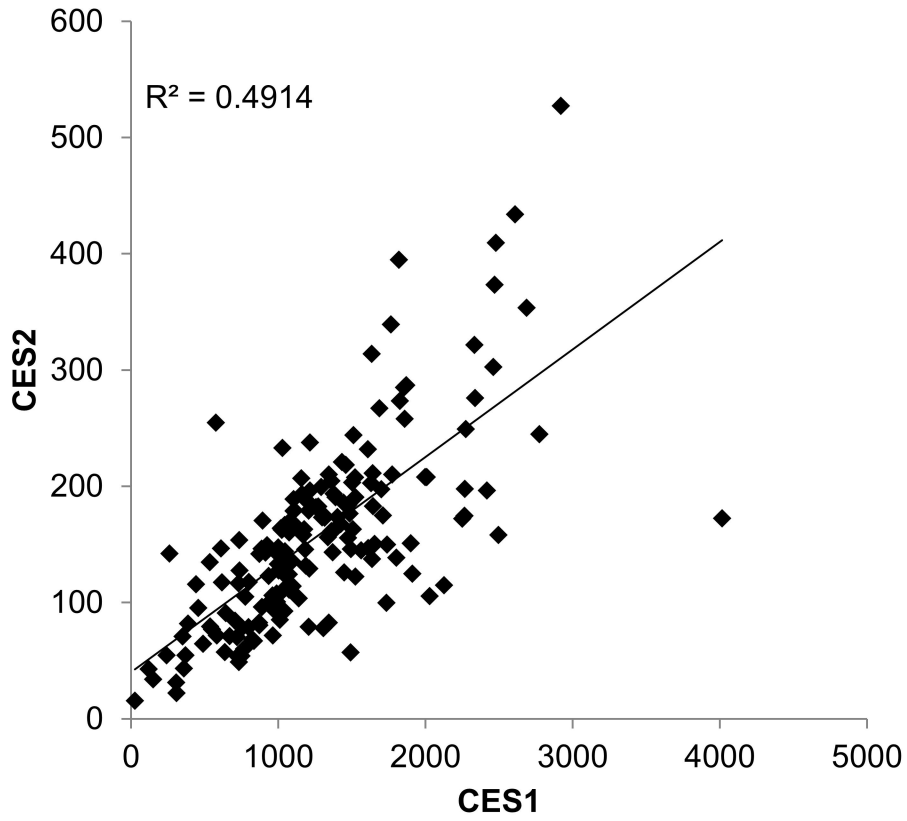

Fig. 5.

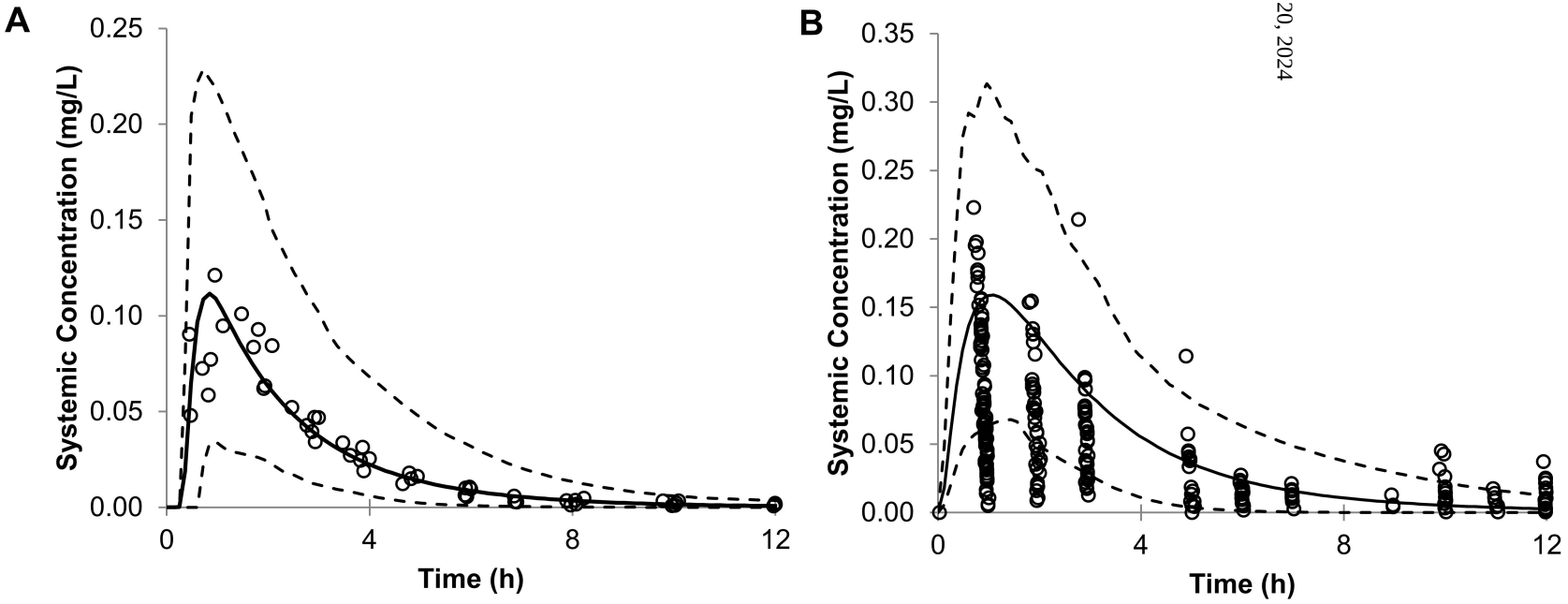

Fig. 6.

SUPPLEMENTARY INFORMATION

Age-dependent absolute abundance of hepatic carboxylesterases (CES1 and CES2) by LC-MS/MS proteomics: Application in prediction of *in vivo* pharmacokinetics of oseltamivir in infants

Mikael Boberg, Marc Vrana, Aanchal Mehrotra, Robin E. Pearce, Andrea Gaedigk, Deepak Kumar Bhatt, J. Steven Leeder and Bhagwat Prasad

Department of Pharmaceutics, University of Washington, Seattle, WA (M.B., M.V., A.M. and B.P.)
Sahlgrenska Academy, University of Gothenburg, Gothenburg, Sweden (M.B.)
Department of Clinical Pharmacology, Toxicology & Therapeutic Innovation, Children's Mercy-Kansas City, MO and School of Medicine, University of Missouri-Kansas City, Kansas City, MO (R.E.P., A.G., J.S.L.)

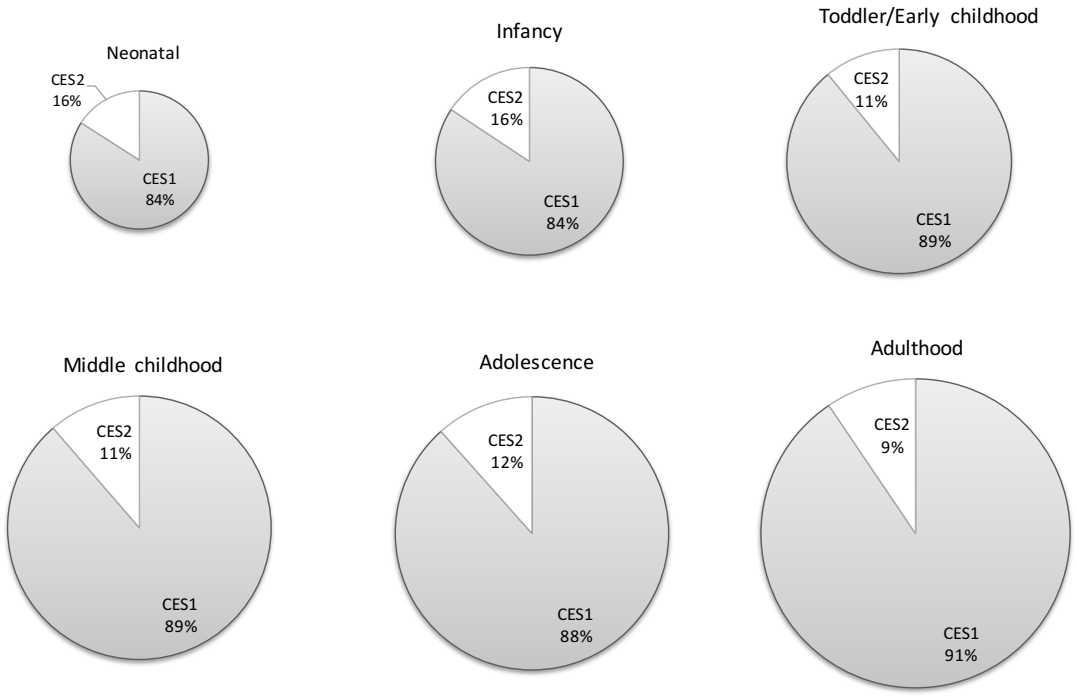

Supplementary Fig. 1S. Relative abundance of CES1 and CES2 during different developmental age groups.

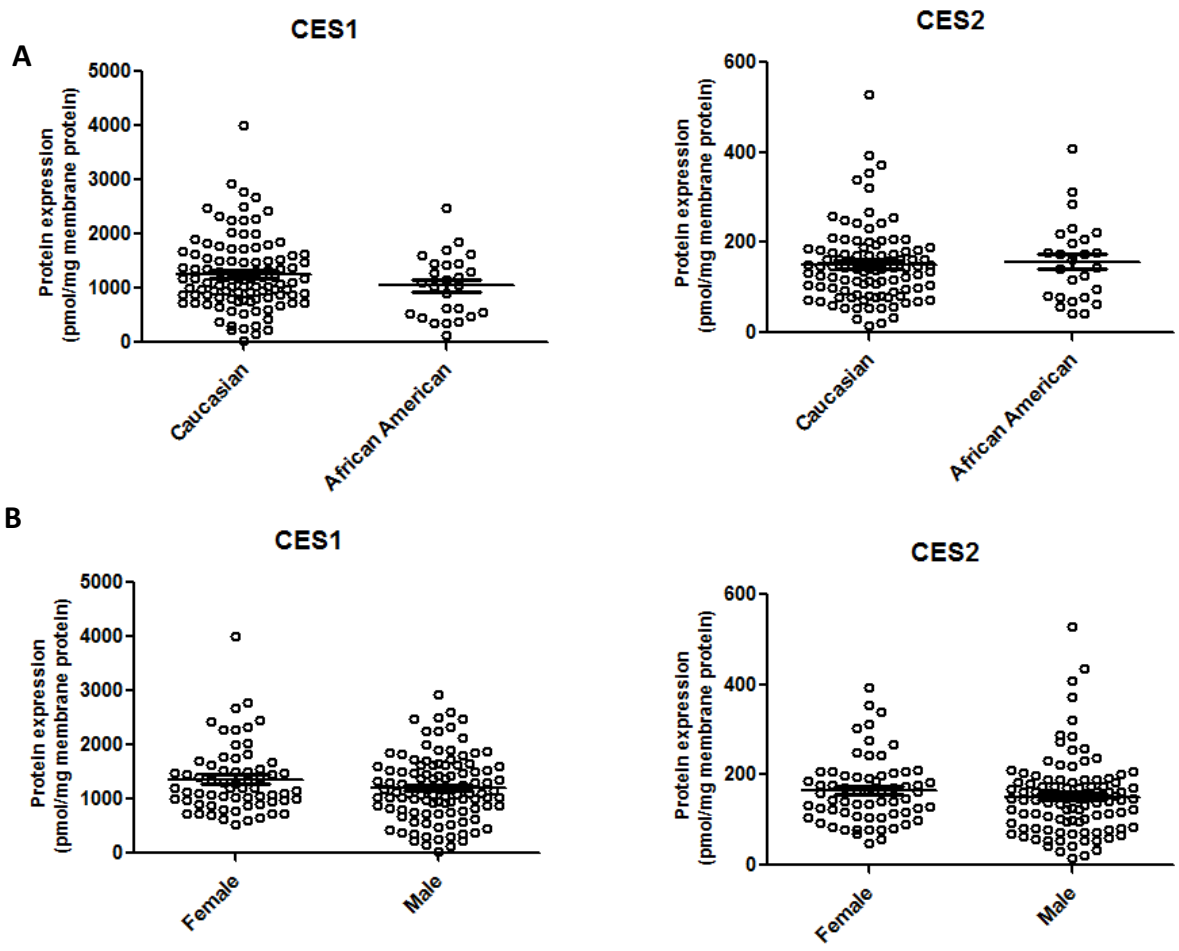

Supplementary Fig. 2S: Effect of ethnicity (A) and gender (B) on CES1 and CES2. Both ethnicity and gender do not show any correlation with protein abundance of CES1 and CES2 in the liver.

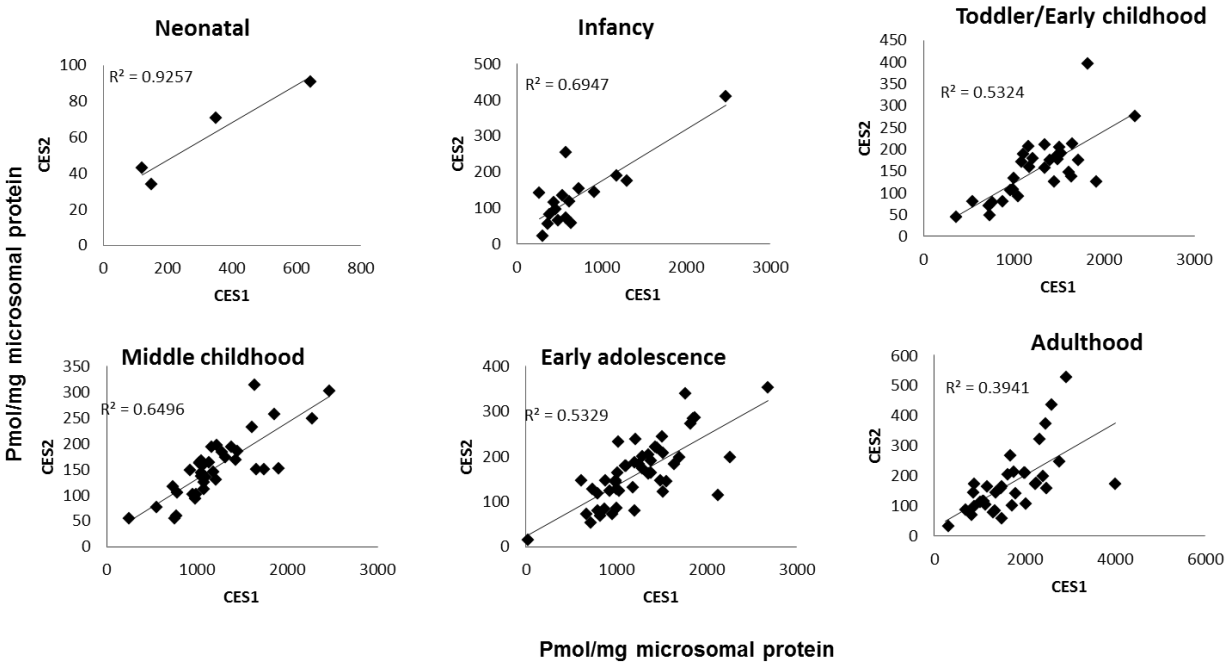

Supplementary Fig. 3S. Correlation of CES1 and CES2 protein expression during different developmental age groups.

Supplementary Table 1S – MRM parameters for analysis of CES1/CES2 peptides and LC gradient programs used for CES1/CES2 peptides and oseltamivir analysis

Protein	Peptide sequence	Light/Heavy	Parent (m/z)	Daughter (m/z)	CE (eV)	DP (V)
CES1	AGQLLSELFTNR	Light	674.865	257.124	33.2	80.3
			674.865	370.208		
			674.865	866.437		
		Heavy	679.869	257.124		
			679.869	370.208		
	EGYLQIGANTQAAQK	Light	796.407	350.135	30.5	89.2
			796.407	888.453		
			796.407	417.246		
		Heavy	800.414	350.135		
			800.414	896.468		
CES2	ADHGDELPFVFR	Light	701.841	1079.552	39	82.3
			701.841	665.377		
			701.841	322.187		
		Heavy	706.845	675.385		
			706.845	332.196		
	TTHTGQVLGSLVHVK	Light	788.944	739.446	37.3	88.6
			788.944	383.24		
			788.944	687.896		
		Heavy	792.951	391.254		
			792.951	691.903		

LC gradient program for analysis of CES1 and CES2

Time (min)	Flow rate (ml/min)	Mobile phase A – Water with 0.1% formic acid (%)	Mobile phase B – Acetonitrile with 0.1% formic acid (%)
0	0.3	97	3
4	0.3	97	3
8	0.3	87	13
18	0.3	70	30
21.5	0.3	65	35
22	0.3	20	80
22.9	0.3	20	80
23	0.3	97	3
26	0.3	97	3

LC gradient program for analysis of oseltamivir

Time (min)	Flow rate (ml/min)	Mobile phase A – Water with 0.1% formic acid (%)	Mobile phase B – Acetonitrile with 0.1% formic acid (%)
0.0	0.3	80	20
0.5	0.3	80	20
1.1	0.3	10	90
1.5	0.3	10	90
2.0	0.3	80	20

Supplementary Table 2S: Demographic information of pediatric and adult liver tissue donors

Clin Pharm ID	Age (yr)	Sex	Ethnicity
432	0.01	Male	Caucasian
780	0.01	Male	African American
271	0.05	Male	African American
1157	0.05	Female	Caucasian
845	0.08	Male	Caucasian
759	0.10	Male	Caucasian
86	0.15	Male	Caucasian
671	0.25	Male	Hispanic
1055	0.26	Male	Caucasian
1296	0.27	Male	African American
1904	0.27	Male	African American
195	0.34	Male	African American
569	0.36	Male	Caucasian
1325	0.50	Female	African American
283	0.54	Male	African American
1281	0.56	Male	African American
1547	0.71	Male	African American
774	0.75	Male	Caucasian
435	0.75	Male	Caucasian
1443	0.91	Female	African American
825	0.92	Male	Caucasian
322	1.00	Male	Hispanic
8926	1.83	Female	Unknown
617	1.95	Female	Caucasian
677	1.97	Male	African American
260	2.00	Male	Caucasian
551	2.00	Male	Caucasian
852	2.00	Male	Hispanic
872	2.00	Male	Caucasian
9101	2.00	Male	Unknown
9023	2.60	Female	Unknown
771	2.75	Male	African American
1791	2.78	Female	African American
346	3.00	Male	Caucasian
866	3.00	Female	Caucasian
9011	3.00	Female	Unknown
9612	3.00	Male	Unknown
372	3.02	Male	Caucasian
1624	3.16	Female	Caucasian
1284	3.34	Female	African American

776	4.00	Female	African American
792	4.00	Male	Native American
9608	4.00	Male	Unknown
9609	4.00	Male	Unknown
451	4.56	Male	Caucasian
4907	4.75	Female	African American
675	5.00	Male	Caucasian
689	5.00	Female	Caucasian
9022	5.00	Unknown	Unknown
9036	5.00	Female	Unknown
71002	5.00	Male	Caucasian
99	6.00	Male	Caucasian
8901	6.00	Female	Unknown
8917	6.00	Female	Unknown
70874	6.00	Male	African American
70921	6.00	Female	Caucasian
71000	6.00	Male	Caucasian
8902	7.00	Male	Unknown
9003	7.00	Female	Unknown
70896	7.00	Male	Caucasian
70898	7.00	Male	Caucasian
70915	7.00	Female	Caucasian
70953	7.00	Female	Caucasian
HL134	7.00	Male	Caucasian
737	7.34	Female	African American
8925	8.00	Male	Unknown
9028	8.00	Female	Unknown
70958	8.00	Unknown	Unknown
71414	8.00	Male	Caucasian
85551	8.00	Male	African American
1860	8.01	Male	Caucasian
356	8.07	Male	African American
1181	8.17	Male	Caucasian
738	8.92	Female	Caucasian
8909	9.00	Female	Unknown
8924	9.00	Female	Unknown
9611	9.00	Male	Unknown
HL113	9.00	Female	Caucasian
HL138	9.00	Female	Caucasian
8703	10.00	Female	Unknown
9006	10.00	Male	Unknown
HL146	10.00	Male	Caucasian
5173	10.76	Female	Caucasian

8920	11.00	Male	Unknown
9013	11.00	Male	Unknown
99377	11.00	Male	Caucasian
HL137	11.00	Male	African American
754	11.54	Female	pacific islander
8906	12.00	Male	Unknown
8912	12.00	Female	Unknown
9027	12.00	Male	Unknown
71307	12.00	Female	Caucasian
85651	12.00	Female	African American
497	12.42	Male	Caucasian
1144	12.64	Female	Unknown
4787	12.87	Male	African American
4925	13.16	Male	African American
1670	13.27	Male	Caucasian
1256	13.86	Male	Caucasian
1908	13.99	Male	Caucasian
613	14.00	Male	Caucasian
326	14.00	Female	Caucasian
8804	14.00	Male	Unknown
8910	14.00	Male	Unknown
9032	14.00	Male	Unknown
9507	14.00	Male	Unknown
620	14.32	Male	African American
4722	14.54	Male	Caucasian
105	14.84	Male	Caucasian
95	15.00	Male	Hispanic
781	15.00	Female	Caucasian
9127	15.00	Male	Unknown
71649	15.00	Female	Caucasian
HL103	15.00	Female	Caucasian
HL139	15.00	Female	Caucasian
4638	15.12	Female	Caucasian
1297	15.22	Male	African American
5242	15.33	Male	Caucasian
811	16.00	Male	Caucasian
70994	16.00	Male	Caucasian
71165	16.00	Female	Caucasian
71281	16.00	Male	Caucasian
142	16.20	Male	Caucasian
4591	16.64	Female	Caucasian
5077	16.71	Female	Caucasian
4906	16.75	Female	Caucasian

596	17.00	Female	Caucasian
885	17.00	Male	African American
8935	17.00	Male	Unknown
9005	17.00	Male	Unknown
9031	17.00	Female	Unknown
9105	17.00	Male	Unknown
85891	17.00	Female	Caucasian
416	18.00	Male	Caucasian
1409	18.00	Male	Caucasian
86461	18.00	Female	Caucasian
HL114	19.00	Male	Caucasian
HL102	21.00	Male	Caucasian
HL105	21.00	Male	African American
HL119	24.00	Male	Caucasian
HL154	26.00	Male	Caucasian
HL111	28.00	Male	Caucasian
HL112	28.00	Male	Caucasian
HL172	28.00	Male	Caucasian
HL125	32.00	Male	Caucasian
HL129	36.00	Female	Caucasian
HL127	38.00	Male	Caucasian
HL136	39.00	Male	Caucasian
HL157	41.00	Female	Caucasian
HL108	42.00	Female	Caucasian
HL168	43.00	Male	Caucasian
HL156	44.00	Male	Caucasian
HL167	44.00	Male	Caucasian
HL133	45.00	Female	Caucasian
HL106	45.00	Female	Caucasian
HL135	45.00	Female	Caucasian
HL171	47.00	Female	Caucasian
HL132	50.00	Female	Caucasian
HL164	50.00	Female	Caucasian
HL115	52.00	Female	Caucasian
HL159	53.00	Female	Caucasian
HL161	53.00	Male	Caucasian
HL163	55.00	Male	Caucasian
HL169	57.00	Male	Caucasian
HL141	59.00	Male	Caucasian
HL166	59.00	Female	Caucasian
HL165	61.00	Male	Asian
HL131	62.00	Female	Caucasian
HL152	64.00	Female	Caucasian

HL160	67.00	Male	Caucasian
HL144	68.00	Female	Caucasian